# INVESTIGATIONS TO ESTABLISH THE INFLUENCE OF THE THERMAL ENERGY FIELD ON SOIL PROPERTIES

SRINIVAS KADALI, SUSHA LEKSHMI S.U., SUSMITA SHARMA and D.N. SINGH

## about the authors

Srinivas Kadali
Indian Institute of Technology Bombay,
Department of Civil Engineering,
Powai, Mumbai-400076, India
E-mail: srinivasciv@gmail.com

Susha Lekshmi S.U.
Indian Institute of Technology Bombay,
Department of Civil Engineering,
Powai, Mumbai-400076, India
E-mail: sushalekshmi.su@gmail.com

Susmita Sharma
Indian Institute of Technology Bombay,
Department of Civil Engineering,
Powai, Mumbai-400076, India
E-mail: susmita.sharma4@gmail.com

**corresponding author**
D.N. Singh
Indian Institute of Technology Bombay,
Department of Civil Engineering,
Powai, Mumbai-400076, India
E-mail: dns@civil.iitb.ac.in

## Abstract

*This paper describes details of a study to investigate and demonstrate the changes undergone by soil when it is exposed to elevated temperatures. Such situations are commonly encountered while designing the foundations for the furnaces, boiler units, forging units, brick kilns, rocket launching pads, buried power-supply cables, air-conditioning ducts, underground explosions, disposal of high-level radioactive and industrial toxic wastes, ground modifications or soil-stabilization techniques, etc. As such, investigations to establish changes undergone by the soil when it is exposed to elevated temperatures assume some importance. With this in view, individual samples of six soils, with entirely different characteristics, were subjected to temperatures up to 300°C (sequentially in steps of 50°C) and after each step of thermal treatment, these samples were characterized for their physical, chemical and mineralogical properties. Based on a critical synthesis of the results, it has been demonstrated that elevated temperatures cause (i) a change in the color, (ii) an increase in the specific gravity, particle size and weight loss, (iii) a reduction in the specific surface area, cation-exchange capacity and zeta-potential, and (iv) a structural transformation of the soil. Though these changes would affect the engineering properties of the soil to a large extent, the scope of this paper is limited to demonstrating the alterations in physical, chemical and mineralogical changes, only, occurring in the soil when it is exposed to elevated temperatures.*

## Keywords

elevated temperatures, soil, characterization, physical characteristics, chemical characteristics, mineralogical characteristics

## NOMENCLATURE

*CEC* = cation-exchange capacity
*DTA* = differential thermal analysis
*EC* = electrical conductivity
*EGME* = ethylene glycol monoethyl ether
*FTIR* = Fourier transform infrared
*FWHM* = full wave half maximum
*LSD* = laser scanning diffraction
*L/S* = liquid-to-solid ratio
*LL* = liquid limit
*OM* = organic matter
*PI* = plasticity index
*PL* = plastic limit
*PLE* = percentage linear expansion
*SL* = shrinkage limit
*SSA* = specific surface area
*TCD* = thermal conductivity detector
*TDS* = total dissolved solids
*TGA* = thermo gravimetric analysis
*USCS* = unified soil-classification system
*XRD* = X-ray diffraction

$XRF$ = X-ray fluorescence
$d$ = lattice spacing
$G$ = specific gravity
$U$ = electrophoretic mobility
$V$ = average linear velocity
$W_a$ = weight of *EGME* absorbed on the soil
$W_s$ = weight of the dry soil
$\lambda$ = wavelength
$\xi$ = zeta-potential
$\eta$ = viscosity
$\phi$ = angle of incidence of the X-rays
$\theta$ = exposure temperature
$\theta_c$ = deviation in temperature with respect to the reference material (i.e., alumina)

## INTRODUCTION

The scenario where soil comes into contact with elevated temperatures (i.e., the thermal energy field) is frequently encountered in various civil-engineering activities. Some of these situations are the design and execution of the foundations for furnaces [1], boiler units, forging units, brick kilns, rocket launching pads, buried power-supply cables and air-conditioning ducts [2], events like volcanic eruptions and activities such as underground explosions, disposal of high-level radioactive [3] and industrial toxic wastes [4], and ground modification or stabilization techniques with the application of chemicals and thermal energy [5-10]. Hence, understanding the influence of elevated temperatures on soil properties becomes necessary. In this context, a brief account of the studies related to this concept, conducted by earlier researchers, is reported in the following.

Farag [4] has reported the use of incineration as a method to treat soil contaminated with the leakage from waste-disposal facilities. Varlakov et al. [3] introduced a heat treatment (between 800 and 1000°C) as an effective solution to decontaminate soils from radioactive and toxic substances. Alcocer and Chowdhury [6] also employed a thermal treatment as a remedy for soils contaminated with crude oil. Earlier researchers [5, 7-9] studied the effect of a heat treatment (300 to 700°C) on clayey bricks. Based on these studies it is clear that the heat treatment of clayey soils (up to 700°C) leads to physical, chemical and microstructural changes, and hence a reduction in their cation-exchange capacity and compressibility. Furthermore, Litvinov [11] and Mitchell [12] have reported that the heat treatment of clayey soils changes their angle of internal friction, cohesion and hence their strength is altered. Also, it has been demonstrated that when soils are exposed to high temperatures, they tend to degrade due to the removal of a significant amount of organic matter [13-16], changes in their specific gravity [17], a reduction in the specific surface area, *SSA*, due to changes in the particle size [18], changes in the consistency limits, an optimum water content and the dry density of the soil [19, 20], volume change characteristics, i.e., shrinkage [21], a variation in the chemical characteristics (viz., cation-exchange capacity, *CEC*, pH and electrical conductivity, *EC*) [22], a deterioration of the structure and porosity, and a considerable loss of nutrients through the volatilization and alteration of soil minerals [23-25]. Though these studies demonstrate that the exposure of soil to elevated temperatures influences its engineering properties (viz., shear strength, compressibility and hydraulic conductivity etc.) to a great extent [26-28], they are (mostly) soil specific and lack a proper explanation regarding the basic mechanism responsible for the alteration of the soil properties when exposed to elevated temperatures.

As such, with an intention to investigate the changes undergone by soils under these circumstances, individual samples of six soils, of entirely different characteristics, were subjected to temperatures up to 300°C, (this being the maximum temperature associated with nuclear wastes [29-30]), sequentially in steps of 50°C. After each step of thermal treatment, these samples were characterized for their physical (viz., appearance, *SSA*, particle size and specific gravity, *G*); chemical (viz., *CEC*, zeta-potential, $\xi$) and mineralogical properties, as described in this paper. Based on a critical synthesis of the results, it has been clearly demonstrated that these properties of the soils are altered when they are exposed to elevated temperatures. Incidentally, as mentioned above, these properties in turn are responsible for controlling the engineering behavior of the soil (viz., shear strength, compressibility, hydraulic conductivity, thermal and chemical stabilization, etc.), to a large extent. However, the scope of this paper is limited to establishing the changes occurring in the soil properties due to their exposure to elevated temperatures, only.

## 2 EXPERIMENTAL INVESTIGATIONS

Two commercially available soils: bentonite and white clay, designated as BT and WC, respectively, from the mines of Gujarat, Western India, were used in this study. In addition, four naturally occurring soils, sampled from a depth of 1 m, from (a) Surat, Gujarat, India, (b) and (c) marine clay from the coast of Mumbai, India, and (d) desert sand from Rajasthan, India, designated as S1, S2, S3 and S4, respectively, were selected for this study. These

six soils in their natural state, and after exposing them to elevated temperatures, were characterized to establish their physical, chemical, mineralogical and thermal properties, details of which are presented in the following.

# 3 PHYSICAL CHARACTERIZATION

## 3.1 SPECIFIC GRAVITY

The specific gravity, *G*, of the soil sample was determined with the help of an ULTRA-PYCNOMETER (Quanta-chrome, USA), available in the Environmental Geotechnology Laboratory, Department of Civil Engineering, IIT Bombay, India, which employs helium gas as the displacing fluid, as per the guidelines provided by the ASTM [31]. The average of two values of the specific gravity, which match with each other quite closely out of three trials, are reported in Table 1.

## 3.2 GRADATIONAL AND CONSISTENCY CHARACTERISTICS

The particle-size distribution of the soil samples (except for soil S4) was determined by employing a hydrometer, as per the guidelines provided by ASTM [32]. In addition, a Laser Scanning Diffraction, *LSD*, particle size analyzer (Beckman Coulter's, LS 13 320, USA), available in the Department of Metallurgical Engineering and Materials Science, IIT Bombay, India, which works on the Polarization Intensity Differential Scattering technique and is capable of covering a particle size range of 0.4 to 2000 μm, was employed for the particle size analysis of the soil samples. Though the amount of sample required for the *LSD* is much less (=1 g), compared to that required for the hydrometer test (=50 g), this methodology has been widely employed for establishing the particle-size distribution characteristics of even coarse-grained soils in an extremely short time [33-34]. In this context, earlier researchers have discussed the limitations associated with the hydrometer analysis for establishing the particle-size distribution characteristics of soils with colloids, organic matter, highly dispersive soil and reactive cement admixtures [35-38]. Earlier researchers [36] have successfully established a comparison of the particle-size distribution characteristics of 'quartz glass beads', obtained from the *LSD* and sieve analysis and an excellent matching between the results has been reported. Hence, *LSD* becomes an obvious choice over the hydrometer analysis.

In order to obtain precise results, and to overcome the limitations associated with an extremely small amount of the soil used for the *LSD*, three trials were conducted and the average of the results was considered as the representative value. However, since each technique involves different assumptions, and defines the size of the particles in a different way, the results (i.e., the percentage finer) would depend on the methodology adopted. The particle size distribution characteristics for various soils are presented in Table 1 and it is clear that there is a good agreement between the results obtained using the two methods for most of the soils considered in the study. The consistency limits (Atterberg limits) of the samples were determined in accordance with the guidelines provided by ASTM [39-40]. Consequently, the soil samples were classified based on the Unified Soil Classification System,

**Table 1**. Physical characteristics of the investigated soils.

| Soil | *G* | *SSA* ($m^2/g$) | Size fraction (%) | | | Atterberg limits (%) | | | | USCS |
|---|---|---|---|---|---|---|---|---|---|---|
| | | | Clay | Silt | Sand | *LL* | *PL* | *PI* | *SL* | |
| BT | 2.73 | 629 | 82 | 18 | - | 305 | 140 | 165 | 30 | CH |
| | | | *78* | *22* | 0 | | | | | |
| WC | 2.63 | 35 | 54 | 46 | - | 54 | 27 | 27 | 17 | CH |
| | | | *59* | *41* | 0 | | | | | |
| S1 | 2.63 | 214 | 39 | 61 | - | 47 | 21 | 26 | 9 | CL |
| | | | 42 | 36 | 22 | | | | | |
| S2 | 2.72 | 135 | 65 | 35 | - | 72 | 30 | 42 | 15 | CH |
| | | | *53* | *47* | 0 | | | | | |
| S3 | 2.69 | 91 | 55 | 45 | - | 45 | 23 | 22 | 8 | CL |
| | | | *41* | *59* | - | | | | | |
| S4 | 2.65 | *7* | - | *2* | 98 | Not applicable | | | | SP |

Note: CH: clay of high plasticity; CL: clay of low plasticity; SP: poorly graded sand numerals in italics are hydrometer results

*USCS* [41]. The test results are presented in Table 1, from which it can be noticed that the soils considered in this study have entirely different characteristics.

### 3.3 SPECIFIC SURFACE AREA

The Specific Surface Area, *SSA*, of the soil samples was determined by using the Ethylene Glycol Monoethyl Ether, *EGME*, method, which has been shown to be the most appropriate method for determining the *SSA* of soils [42-44]. The set-up available in the Environmental Geotechnology Laboratory, Department of Civil Engineering, IIT Bombay, India, was employed for this purpose. A total of 2 g of air-dried soil sample was spread uniformly on the bottom of a glass petri dish, which is 40 mm in internal diameter, 2 mm thick and 20 mm high, and covered with a perforated watch-glass. Six such dishes, with a sample in them, were placed in a vacuum desiccator that contained 250 g of $P_2O_5$ and helped to maintain a constant vapor pressure. The sample was evacuated by applying vacuum (0.03 mbar) for 2 h, weighed and replaced in the desiccator. This process was repeated several times and stopped when three consecutive weights were found to be almost same. Later, 6 ml of analytical grade EGME solution was added to the sample and the mixture was swirled, gently, until it became a slurry. This slurry was then placed in the desiccator over a desiccant (mixture of 100 g $CaCl_2$ and 20 ml EGME) for 12 h, which helped in maintaining constant conditions that are just sufficient to form a monolayer. The initial weight of the slurry along with the glass dish was measured using a precision balance and the dish was replaced in the desiccator for evacuation. The glass dish was taken out of the desiccator, weighed and re-placed in it several times, until it attained a constant weight. The amount of EGME ($W_a$, in g) that was absorbed per gram of the sample ($W_s$, in g), corresponding to this constant weight condition, was computed by subtracting the dry weight of the sample from the weight of the EGME mixed sample. Subsequently, by employing Eq. 1, the *SSA* of the sample was determined [42-44] and the results are presented in Table 1.

$$SSA = W_a \cdot \left(0.000286 \cdot W_s\right)^{-1} \qquad (1)$$

## 4 CHEMICAL CHARACTERIZATION

### 4.1 CHEMICAL COMPOSITION

The chemical composition of the soil samples, in the form of major oxides, was determined using an X-Ray Fluorescence set-up, XRF (Phillips 1410, Netherlands), available at the Sophisticated Analytical and Instrumentation Facility, SAIF, IIT Bombay, India. A finely powdered soil sample weighing 4 g and 1 g of microcrystalline cellulose were mixed thoroughly with 2 ml of isopropyl alcohol and the mixture was kept below an infrared lamp for slow drying until it became a powder. Subsequently, this powder was poured into an aluminum dish (with an inner diameter of 33 mm and a height of 12 mm) containing methyl-cellulose powder (supplied by Merck Chemicals, India) up to about 70 % of the volume of the dish. To make a pellet, the dish was compressed with the help of a hydraulic jack by applying a load of 15 tonnes. The physical calibration of the XRF set-up, which is conducted to eliminate the error resulting from an uneven and slanting base line, was made using a standard reference material (SRM) supplied by UGCS, USA. While the chemical calibration of the instrument was performed using an international standard reference material, [Fly ash (2689, 2690, 2691), cements (354, 372, 372/1) and soils (SO-2,SO-3,SO-4)], procured from NIST, USA. The chemical composition of the sample was determined by mounting the pellet in the sample holder of the XRF set-up and the results are presented in Table 2.

### 4.2 CATION-EXCHANGE CAPACITY

The cation-exchange capacity, *CEC*, is the property of the soil by which certain cations adsorbed on the soil particles get replaced by other cations [45-48]. The capacity of a soil to hold cations mainly depends on the

**Table 2**. Chemical composition (% by weight) of the investigated soils.

| Soil | $SiO_2$ | $Al_2O_3$ | $Fe_2O_3$ | CaO | $K_2O$ | $Na_2O$ | $TiO_2$ | MgO | $P_2O_5$ |
|---|---|---|---|---|---|---|---|---|---|
| BT | 42.06 | 18.90 | 31.17 | 1.11 | 0.35 | 3.55 | 1.36 | 0.96 | 0.11 |
| WC | 37.94 | 52.84 | 2.52 | 1.59 | 1.84 | 0.19 | 2.69 | 0.20 | 0.03 |
| S1 | 37.98 | 30.70 | 14.96 | 8.92 | 0.91 | 1.65 | 2.26 | 2.16 | 0.11 |
| S2 | 42.22 | 18.53 | 16.13 | 11.47 | 3.73 | 4.19 | 1.45 | 1.73 | 0.27 |
| S3 | 39.92 | 27.81 | 8.55 | 11.39 | 3.51 | 5.36 | 0.76 | 2.27 | 0.23 |
| S4 | 66.00 | 16.99 | 11.59 | 0.04 | 4.39 | 0.12 | 0.36 | 0.22 | 0.13 |

pH and the ionic strength of the soil-fluid system. The guidelines presented in the literature [47] were followed to determine the *CEC* of the soil samples used in this study by employing the test set-up available in the Environmental Geotechnology Laboratory, Department of Civil Engineering, IIT Bombay, India.

The soil weighing 1 g was transferred to a 1-ml round-bottom and narrow-neck centrifuge tube and 9 ml of 1N $CH_3COONa$ was added to it. This mixture was shaken on a mechanical shaker for 5 min and later centrifuged until the supernatant was clear. The supernatant was decanted and this process was repeated three times on the residues. Subsequently, 9 ml of 99% isopropyl alcohol was added to the residues and shaking on a mechanical shaker, for 5 min, was performed. This mixture was centrifuged until the supernatant became clear and this procedure was repeated two more times. In addition, 9 ml of $CH_3COONH_4$ was added to the residues and this mixture was shaken in a mechanical shaker for 5 min. This mixture was centrifuged until the supernatant became clear. Following this, the supernatant was decanted into a 100-ml flask and the procedure with the $CH_3COONH_4$ was repeated twice. Finally, the combined supernatant was diluted and brought to 100 ml volume by adding $CH_3COONH_4$ . The $Na^+$ concentration was obtained by employing Inductively Coupled Plasma–Atomic Emission Spectrometry (ARCOS, M/s. SPECTRO, Germany). The *CEC* of the sample was computed by employing Eq. 2 and the results are presented in Table 3.

$$CEC = \frac{\text{Concentration of Na}\left(\frac{\mu\text{g}}{\text{ml}}\right) \times 100 \times \text{Vol. of extract(ml)}}{\text{The molar weight of Na} \times 1000 \times \text{wt. of sample(g)}} \quad (2)$$

**Table 3**. Chemical characteristics of the investigated soils.

| Soil | pH | *EC* (μS/cm) | *TDS* (ppm) | *ξ* (mV) | *CEC* (meq./100g) |
|---|---|---|---|---|---|
| BT | 7.78 | 176.4 | 88 | 36.4 | 108.33 |
| WC | 7.63 | 94 | 47.1 | 17.5 | 14.77 |
| S1 | 7.86 | 145 | 72.5 | 27.6 | 45.54 |
| S2 | 7.82 | 520 | 260.8 | 30.6 | 30.77 |
| S3 | 7.61 | 730 | 364.2 | 27.6 | 26.90 |
| S4 | 7.89 | 205 | 101 | 14.5 | 3.46 |

## 4.3 ZETA POTENTIAL

In order to investigate the influence of pore fluid on the particle-to-particle interaction within the soil mass, a determination of the change in the surface-charge potential of the particles, which is indirectly defined as the zeta potential, *ξ*, is quite useful [49-52]. Hence, the *ξ* for the soil samples used in this study was determined by employing an automated electrophoresis instrument (Zetasizer-Nano series, Malvern instruments, United Kingdom), available at the Sophisticated Analytical and Instrumentation Facility, SAIF, IIT Bombay, India. This instrument works on the light-scattering technique, which determines the electrophoretic mobility, *U*, which is the velocity of a particle in the solution produced by an external electric field of a certain strength. This *U* can be used to compute *ξ* by employing Helmoltz-Smoluchowski theory, which in the mathematical form can be represented by Eq. 3 [53].

$$\xi = \frac{4\pi\eta U}{\varepsilon} \quad (3)$$

where $\eta$ is the viscosity of the soil solution (Pa·s), $\varepsilon$ is the dielectric constant of the soil solution and *U* is the electrophoretic mobility [μm.cm / (V·s)].

Measurements were conducted on 2 ml of soil suspension, by maintaining a liquid-to-solid ratio, *L/S*, equal to 100 (corresponding to 25°C), by following the guidelines provided by Kaya et al.[53]. Furthermore, the pH, Electrical Conductivity, *EC*, and Total Dissolved Solids, *TDS*, of the soil were measured by employing a water-quality analyzer (Model PE 136, Elico Ltd., India), available in the Environmental Geotechnology Laboratory, Department of Civil Engineering, IIT Bombay, India, and the results are presented in Table 3.

## 4.4 ORGANIC CONTENT ANALYSIS

The presence of the organic matter, *OM* (in percentage by weight), in the soil samples was determined by using a Carbon, Hydrogen, Nitrogen and Sulphur analyzer (CHNS analyzer, make FLASH EA 1112 series, Thermo Finnigan, Italy), available at the Sophisticated Analytical and Instrumentation Facility, SAIF, IIT Bombay, India. This instrument works on the principle of the "Dumas method", which involves complete and instantaneous oxidation of the sample (4-5 mg weight) by employing "flash combustion" at 900°C. The combustion products ($CO_2$, $H_2O$, $NO_2$ and $SO_2$) were separated by a chromatographic column and detected with the help of a thermal conductivity detector, *TCD*. The *TCD* yields an output signal that is proportional to the concentration of the individual components of the soil mixture. This instrument, which finds its role in determining C, H, N and S in organic compounds, was calibrated by analyzing compounds with K-factors calculations, as suggested by the manufacturer. By using this instrument, the

elements belonging to the CHNS/O group and present in the soils can be detected simultaneously. The value of the *OM* for different soils is listed in Table 4.

**Table 4**. The organic matter (% by weight) in the investigated soils.

| Soil | C | H | N | S | Total |
|---|---|---|---|---|---|
| WC | 0.552 | 1.144 | 0.033 | NIL | 1.729 |
| BT | 0.158 | 1.5 | 0.064 | NIL | 1.722 |
| S1 | 1.393 | 0.704 | 0.015 | NIL | 2.111 |
| S2 | 2.085 | 0.47 | 0.077 | NIL | 2.632 |
| S3 | 2.146 | 0.38 | 0.029 | NIL | 2.555 |
| S4 | 0.958 | 0.091 | 0.003 | NIL | 1.051 |

### 4.5 FOURIER TRANSFORM INFRARED SPECTROMETER (FTIR) STUDIES

*FTIR* studies are found to be quite useful for the identification of the chemical bonds (functional groups) present in the soil, which are representative of the soil contamination [54-55]. Spectrographs of the soils were captured by employing a Fourier Transform Infrared Spectrometer (Nicolet Instruments Corporation, USA; Model: MAGNA 550; Range 4000 $cm^{-1}$ to 500 $cm^{-1}$), available at the Sophisticated Analytical and Instrumentation Facility, SAIF, IIT Bombay, India. A small quantity of the soil in powder form (weighing 2 mg) was mixed uniformly with KBr and pelletized into a transparent disk by applying a 3 T loading. The pellet was irradiated with the IR beam for the complete range of the wave numbers, mentioned above, and the intensity of the IR radiation that was absorbed and/or transmitted was recorded. Though the amount of sample used for this analysis is limited, the application of FTIR studies for detecting the presence of chemical bonds in the soil samples is well established [54-55].

## 5 MINERALOGICAL CHARACTERIZATION

The mineralogical composition of the soils was determined with the help of an X-ray diffraction spectrometer (Phillips, Eindhoven, Netherlands), available in the Department of Metallurgical Engineering and Materials Science, IIT Bombay, India, which is fitted with a graphite monochromator and employs Cu-Kα as the source. The minerals present in the soil sample were identified with the help of the Joint Committee on Powder Diffraction Standards, JCPDS [56] search files, from the diffractograms, and are listed in Table 5. It is clear from the table that the soil samples consist of a wide range of minerals, except for Soils S2 and S3. It is worth mentioning here

**Table 5**. Mineralogical composition of the investigated soils.

| Soil | Minerals |
|---|---|
| BT | Montmorillonite, Muscovite |
| WC | Kaolinite, Illite |
| S1 | Montmorillonite, Quartz, Calcite |
| S2, S3 | Montmorillonite, Calcite, Muscovite, Quartz |
| S4 | Quartz |

that quantification (i.e., the percentage by weight) of various minerals present in the soils can be made using the appropriate software (i.e., Reitveld) [57-58]. However, due to non-availability of such software, the quantification of the amount of various minerals present in the soils used in the present study could not be conducted.

## 6 THERMAL CHARACTERIZATION

### 6.1 LINEAR EXPANSION

The percentage linear expansion, *PLE*, of the soil samples due to heating was determined by employing a dilatometer (Orton, DIL2016 STD, USA) available in the Department of Metallurgical Engineering and Materials Science, IIT Bombay, India. The sample of 12 mm in diameter and 14 mm in length was prepared by pressurizing the finely powdered, air-dried (viz., the ambience being 27±1°C and 60±2 % relative humidity) soil sample in a mold and by applying a load of 3 tonnes, which helps in binding the soil grains. Subsequently, this sample was placed in the dilatometer and a deformation measuring device was attached to it. Furthermore, the sample was heated up to 600°C, at a constant rate of 10°C/min., and the *PLE* was data-logged with respect to the temperature, θ, and results are shown in Fig. 1.

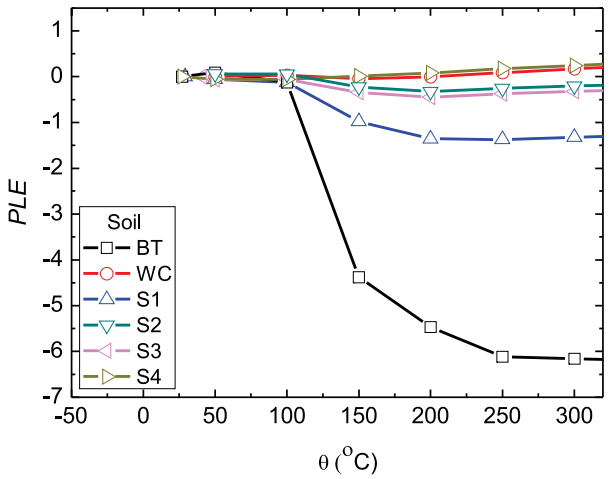


**Figure 1**. Variation of *PLE* with temperature.

### 6.2 THERMO GRAVIMETRIC ANALYSIS (TGA)

Thermo gravimetric analyses of the soil samples were conducted with the help of a thermo gravimetric analyzer (Model Diamond TG/DTA, Perkin Elmer, USA), available at the Sophisticated Analytical and Instrumentation Facility, SAIF, IIT Bombay, India, to determine their response (i.e., the percentage weight loss with respect to the original weight, 20 mg) when exposed to elevated temperatures up to 300°C, by maintaining a rate of heating of 10°C per minute. During the analysis, a controlled environment (i.e., an inert gas, $N_2$, flowing at a rate of 600 ml/min, under vacuum $10^{-2}$ Torr) was maintained for monitoring the thermal stability of the sample. It should be noted that this analysis permits the simultaneous quantification of the bound water, biodegradable and humic components in one simple analytical process in the temperature ranges 25 to 190°C, 190 to 450°C and 450 to 650°C, respectively.

### 6.3 DIFFERENTIAL THERMAL ANALYSIS (DTA)

Differential thermal analyses of the soil samples were conducted, maintaining the same conditions as mentioned for the TGA analysis, with the help of a differential thermal analyzer (Model Diamond TG/DTA, Perkin Elmer, USA), available at the Sophisticated Analytical and Instrumentation Facility, SAIF, IIT Bombay, India. This analysis helps in estimating the endothermic or exothermic behaviors of the sample by recording the difference in the temperatures between the sample (weighing 20 mg) and a reference material (viz., Alumina) heated up to 300°C by maintaining the rate of heating as 10°C/min with the help of a set of thermocouples [59-60].

## 7 RESULTS AND DISCUSSION

### 7.1 PHYSICAL APPEARANCE

Figure 2 shows the changes in the physical appearance of the soil samples when exposed to elevated temperatures. It can be seen from the figure that up to θ≤250°C there is no appreciable change in the color of the soil sample. However, for θ>250°C and except for the Soil WC (white colored), the color of the samples changes from brown/grey to brownish/reddish, which can be attributed to increased oxidation and other chemical changes (i.e., shifting of the absorption bands and the disappearance of the absorption features observed in the FTIR spectra, as defined in the following). Kampf et al. [61] and Schwertmann [62] observed a link between the increased

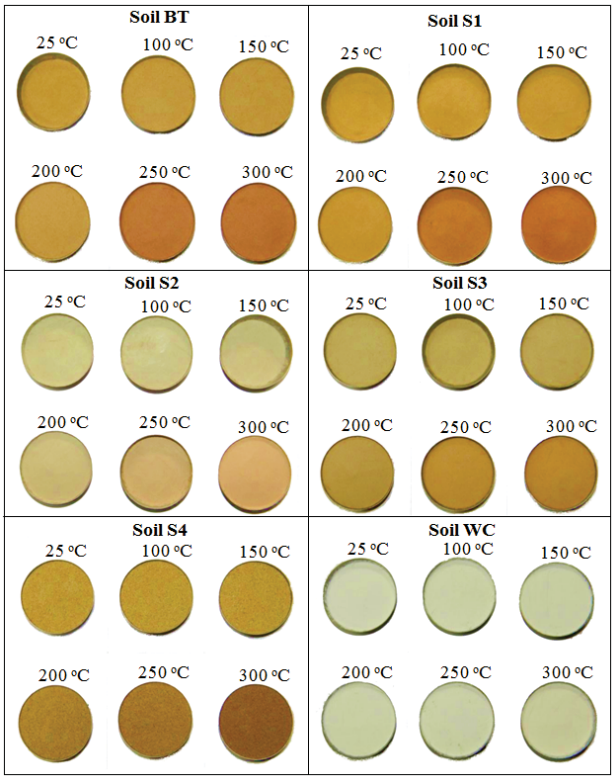


**Figure 2.** Changes in the color of investigated soils due to heating.

redness and the transformation of iron oxides due to the exposure of the soil to elevated temperatures. In this context, some other researchers [14, 63] suggested that even dark-grey color soils (viz., Soil S2) containing limited organic matter, ferrous and manganese compounds, elemental carbon and hematite would also exhibit a change in the color due to their exposure to elevated temperatures. In contrast, Soil WC, due to the presence of a substantial amount of $Al_2O_3$ (≈52.3%, refer Table 2), does not exhibit any change in color on exposure to elevated temperatures.

### 7.2 SPECIFIC GRAVITY

Figure 3 shows the change in the specific gravity, *G*, of different soil samples with respect to the exposure temperature. It is evident from the plot that an increase in *G* due to heating is much more for Soils BT, S2 and S3 than for their counterparts (i.e., Soils WC, S1 and S4). The change in *G* can be attributed to the shrinkage undergone by the soil particles, due to the complete removal of the absorbed water, as depicted in Fig. 1. At higher temperatures the finer particles tend to agglomerate, which also leads to a change in the *G* value. However, the exposure of the soil to elevated temperatures is responsible for a decrease in the clay-sized and

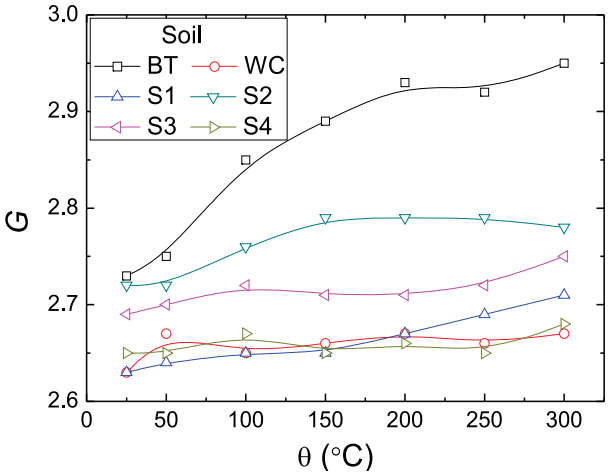


**Figure 3**. Variation of Specific Gravity of investigated soils with temperature.

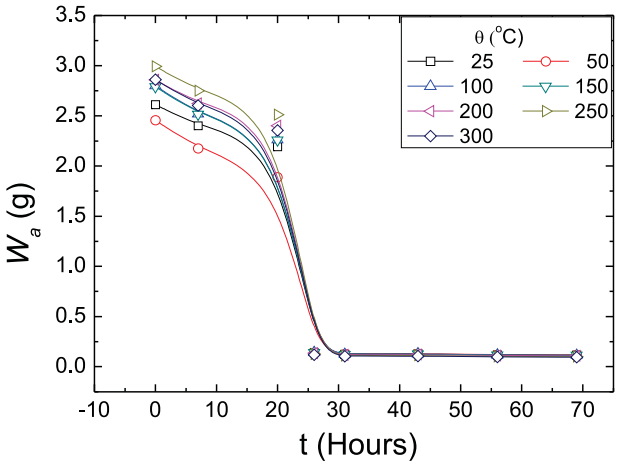


**Figure 4**. Variation of $W_a$ with time for Soil S1.

the silt-sized fractions of the soils, except for the Soil S4, which mainly consists of quartz, a mineral insensitive to temperature variations considered in this study. This observation is consistent with the findings reported by Yilmaz [17], which reveal that for θ≥100°C, some soils exhibit tremendous changes in the specific gravity, which could be attributed to a loss of moisture, organics, impurities and changes occurring at the elemental level. Incidentally, in contrast to these findings, other researchers [20] have reported a decrease in the specific gravity with an increase in the temperature for highly plastic clays form Turkey.

## 7.3 SPECIFIC SURFACE AREA

Following the methodology for determining the *SSA*, mentioned earlier, the weight of the *EGME* retained on the soil particles, $W_a$, (used for a calculation of the *SSA* of a soil sample by employing Eq. 1) was recorded with respect to time for all the soils considered in this study. However, for the sake of brevity, the response of Soil S1 is presented in Fig. 4. Following this methodology, the *SSA* of different soils, treated at temperatures ranging from 25 to 300°C, was determined and the results are listed in Table 6. The data presented in the table reveals a decrease in the *SSA* of the soil sample with an increase in the temperature, which is prominent for the Soils WC and S4, as compared to their counterparts (i.e., Soils BT, S1, S2 and S3). This, in general, can be attributed to the depletion of organic matter from the soil due to its exposure to elevated temperatures. Such changes in the *SSA* can be further substantiated by changes occurring in the particle size of the soils, due to elevated temperatures, as described below.

**Table 6**. *SSA* (in $m^2/g$) of investigated soils at elevated temperature.

| θ (°C) | Soil | | | | | |
|---|---|---|---|---|---|---|
| | BT | WC | S1 | S2 | S3 | S4 |
| 25 | 629 | 35 | 214 | 135 | 91 | 7 |
| 50 | 623 | 32 | 209 | 135 | 87 | 6 |
| | *0.95* | *8.57* | *2.34* | *0* | *4.40* | *14.29* |
| 100 | 585 | 31 | 210 | 126 | 88 | 5 |
| | *7.00* | *11.43* | *1.87* | *6.67* | *3.30* | *28.57* |
| 150 | 579 | 25 | 202 | 128 | 81 | 5 |
| | *7.95* | *28.57* | *5.61* | *5.19* | *10.99* | *28.57* |
| 200 | 576 | 24 | 193 | 121 | 78 | 4 |
| | *8.43* | *31.43* | *9.81* | *10.37* | *14.29* | *42.86* |
| 250 | 577 | 19 | 180 | 118 | 75 | 4 |
| | *8.27* | *45.71* | *15.89* | *12.59* | *17.58* | *42.86* |
| 300 | 572 | 12 | 170 | 92 | 72 | 4 |
| | *9.06* | *65.71* | *20.56* | *31.85* | *20.88* | *42.86* |

Note: Numerals in italics represent the % change with respect to the value at 25°C

## 7.4 PARTICLE SIZE ANALYSIS

The results of the particle size analysis, obtained by resorting to *LSD*, on the soil samples exposed to different temperatures, are shown in Fig. 5. From the trends in the figure, it is clear that all the soils, except for Soil S4, exhibit a change in the particle diameter (i.e., there is a scatter around the dotted line, which represents the soil at normal temperature) with an increase in the exposure temperature. In general, it has been noted that at higher temperatures (particularly

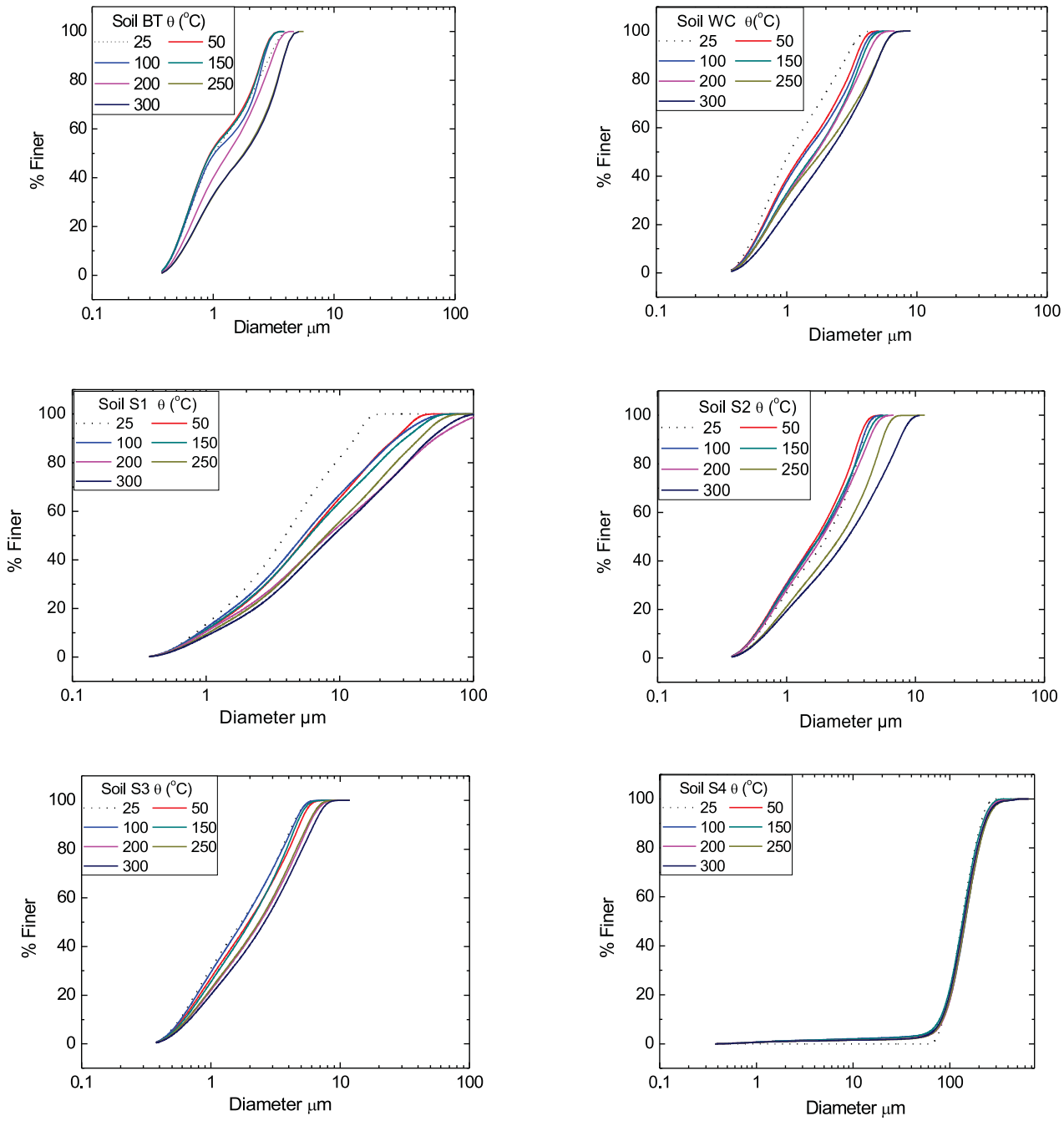


**Figure 5**. Variation of the particle size distribution characteristics of the investigated soils (obtained from *LSD*) with temperature.

for θ>200°C) the tendency of the soil particles is to expand. However, this expansion is observed to be much less for Soil S4 (which is a sandy soil) than for its counterparts.

Based on the *LSD* analysis, the particle sizes of the soils corresponding to the clay-sized (<2 μm) and the silt-sized (2 to 75 μm) fractions were determined and plotted with respect to the temperature, θ, (refer Fig. 6). It is clear from the trends presented in Fig. 6 that, in general, except for Soil S4, the clay-sized fraction decreases while the silt-sized fraction increases with an increase in temperature. This further substantiates the findings, as reported above, that exposure of the soil to elevated temperatures results in an increase in its particle size. However, the Soil S4 with passive minerals (viz., predominance of quartz in Soil S4) was found to be insensitive to temperature variations.

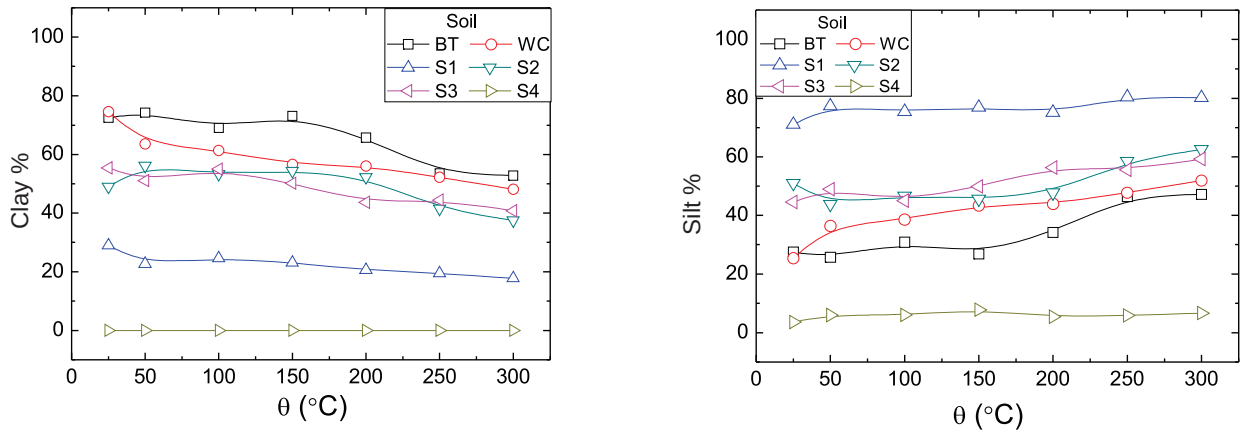


**Figure 6**. Variation of the percentage clay and silt fractions of the investigated soils with temperature.

## 7.5 CATION-EXCHANGE CAPACITY

The Cation-exchange capacity, *CEC*, of the soil samples is listed in Table 7. The numerals in italics represent the percentage change in the *CEC* with respect to its value at 25°C. It can be seen that the *CEC* of the soil samples decreases as the temperature increases [45-48]. This can be attributed to a reduction in the exchangeable cations and a loss of organic matter present in the soil. A decrease in the *CEC* value of the heated soil sample can also be justified by an increase in the particle size and a decrease in the *SSA* when soil is exposed to high temperatures, as discussed above.

## 7.6 ZETA POTENTIAL

The changes in the zeta-potential, $\xi$, with respect to the temperature, θ, are presented in Table 8. A decrease in the particle mobility (i.e., $\xi$ becomes less negative) was observed when the temperature increases from 25 to 300°C. This is consistent with the observations reported by Chorom and Rengasamy [64]. A reduction in $\xi$ when the soil is subjected to heating, as depicted in Table 8, can be attributed to the charge reduction caused by the reduction in the *CEC* (see Table 7) and the structural changes in the crystal lattice due to an increase in the *d*-spacing, as explained in the following (section *XRD*

**Table 7**. *CEC* (in meq./100g) of the investigated soils at elevated temperatures.

| θ (°C) | Soil | | | | | |
|---|---|---|---|---|---|---|
| | BT | WC | S1 | S2 | S3 | S4 |
| 25 | 108.33 | 14.77 | 45.54 | 30.77 | 26.90 | 3.46 |
| 50 | 105.28 | 14.35 | 43.68 | 30.18 | 26.35 | 3.42 |
| | *2.82* | *2.84* | *4.08* | *1.92* | *2.04* | *1.16* |
| 100 | 104.67 | 13.97 | 42.49 | 29.92 | 23.70 | 3.32 |
| | *3.38* | *5.42* | *6.70* | *2.76* | *2.04* | *4.05* |
| 150 | 101.19 | 13.81 | 41.84 | 29.31 | 23.03 | 3.31 |
| | *6.59* | *6.50* | *8.12* | *4.74* | *14.39* | *4.34* |
| 200 | 96.75 | 11.55 | 29.71 | 29.14 | 20.28 | 3.28 |
| | *10.69* | *21.80* | *34.76* | *5.30* | *24.61* | *5.20* |
| 250 | 95.68 | 11.11 | 28.10 | 28.10 | 19.74 | 2.07 |
| | *11.68* | *24.78* | *38.30* | *8.68* | *26.62* | *40.17* |
| 300 | 95.28 | 10.97 | 27.42 | 28.10 | 19.68 | 1.61 |
| | *12.05* | *25.73* | *39.79* | *8.68* | *26.84* | *53.47* |

Note: Numerals in italics represent the % change with respect to the value at 25°C

**Table 8**. Zeta-Potential, $\xi$, (- mV) of the investigated soils at elevated temperatures.

| θ (°C) | Soil | | | | | |
|---|---|---|---|---|---|---|
| | BT | WC | S1 | S2 | S3 | S4 |
| 25 | 36.4 | 17.5 | 27.6 | 30.6 | 27.6 | 14.5 |
| 50 | 33.4 | 17.5 | 27.4 | 30.8 | 26.4 | 14.4 |
| | *8.24* | *0* | *0.72* | *-0.65* | *4.35* | *0.69* |
| 100 | 34.4 | 16.6 | 26.6 | 30.1 | 26.2 | 14.3 |
| | *5.49* | *5.14* | *3.62* | *1.63* | *5.07* | *1.38* |
| 150 | 34.1 | 15.9 | 26.2 | 29.6 | 25.5 | 14.3 |
| | *6.32* | *9.14* | *5.07* | *3.27* | *7.61* | *1.38* |
| 200 | 34.1 | 14.2 | 25.9 | 29.5 | 25.3 | 13.8 |
| | *6.32* | *18.86* | *6.16* | *3.59* | *8.33* | *4.83* |
| 250 | 33.3 | 12.3 | 25.7 | 28.1 | 24.4 | 12.7 |
| | *8.51* | *29.71* | *6.88* | *8.17* | *11.59* | *12.41* |
| 300 | 34.6 | 11.0 | 23.9 | 22.9 | 22.9 | 11.4 |
| | *4.95* | *37.14* | *13.41* | *25.16* | *17.03* | *21.38* |

Note: Numerals in italics represent the % change with respect to the value at 25°C

analysis), and an expansion of the soil minerals with temperature (refer Fig. 1). Furthermore, the $\xi$ of the soil can decrease due to a decrease in the various attributes of the soil (viz., electrical conductivity, specific surface area and particle size distribution).

## 7.7 FOURIER TRANSFORM INFRARED SPECTROMETER (FTIR) ANALYSIS

The FTIR spectral characteristics of the soil samples were obtained by plotting the transmittance (in %) with respect to the wave number, $cm^{-1}$, as depicted

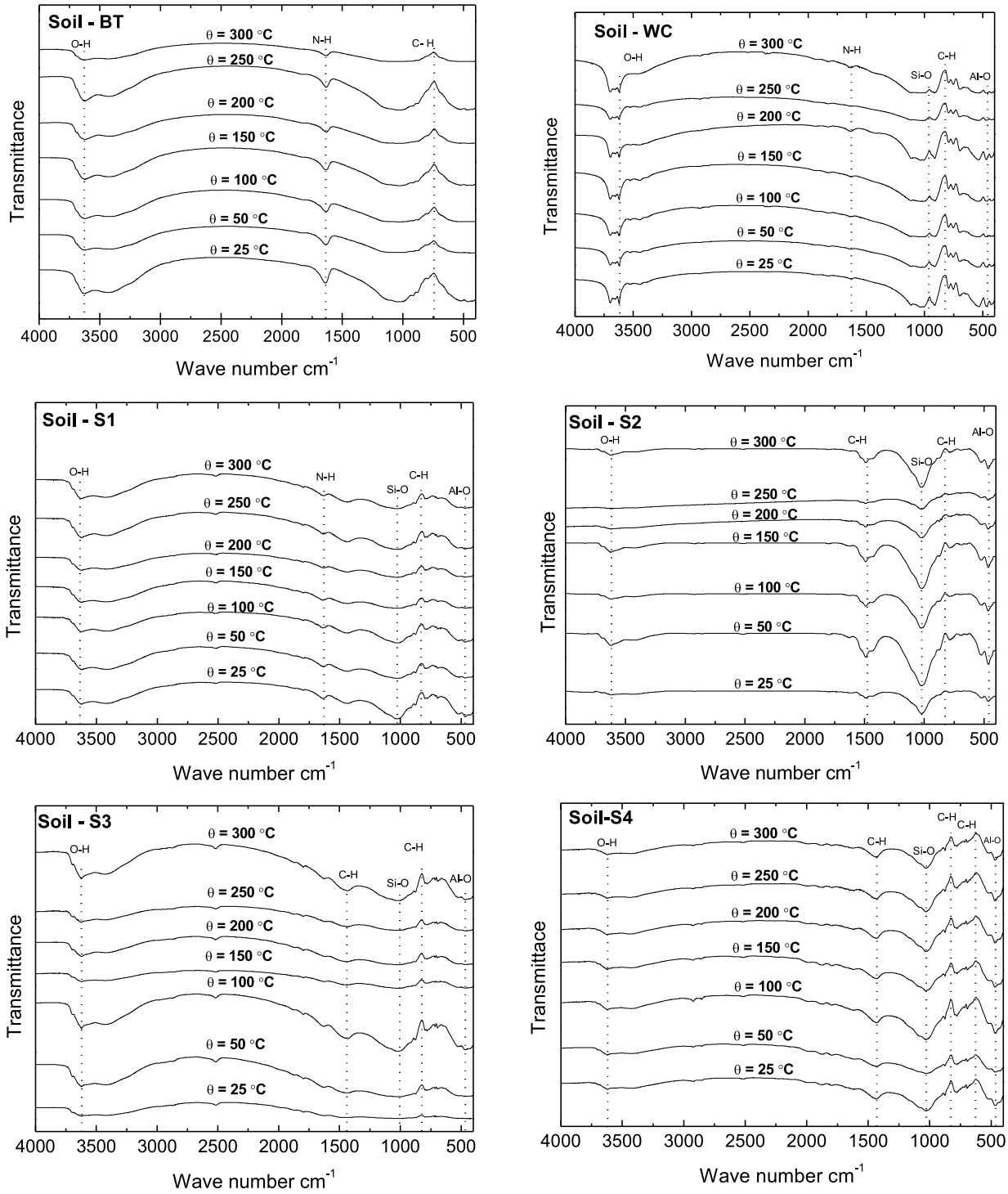


**Figure 7**. FTIR spectra of soils heated at the investigated temperatures.

in Fig. 7. The resultant trend shows that there is not much variation in the spectral characteristics of the samples due to their exposure to elevated temperatures. Furthermore, this analysis reveals that the O-H bonds (3628, 3615, 3635, 3613, 3631 and 3622 $cm^{-1}$ for Soils BT, WC, S1, S2, S3 and S4, respectively), the N-H bonds (1636, 1635, 1627, 1030 $cm^{-1}$ for Soils BT, WC, S1 and S4, respectively), the C-H bonds (740, 831, 825, 833 & 1471, 828 & 1440, 829 & 640 $cm^{-1}$ for Soils BT, WC, S1, S2, S3 and S4, respectively), and the Si-O and Al-O bonds (1000-1260 $cm^{-1}$and 400-1000 $cm^{-1}$, for soils WC, S1, S2, S3 and S4, respectively) are present in the soils considered in this study. The existence of the O-H bond is due to the hygroscopic moisture, which is present in the samples both before and after the exposure to elevated temperatures, whereas the C-H and C-N bonds are mainly due to the presence of organic matter in the soil, which might be eliminated completely corresponding to θ≥300°C. However, it should be noted that complete removal of the C-H and C-N bonds occurs at temperatures higher than 300°C. The peaks in the FTIR plots, corresponding to the temperature range considered in this study, indicate 'flattening' (see Fig. 7), which represents the sequential removal of the C-H and C-N bonds.

## 7.8 X-RAY DIFFRACTION ANALYSIS

The six soil samples were exposed to 300°C, sequentially in steps of 50°C, and their *XRD* patterns are presented in Fig. 8. From these patterns it can be clearly observed that the peaks are shifted, towards the left, with an increase in the exposure temperature. This indicates a decrease in 2ϕ (where ϕ is the angle of incidence of the X-rays) with an increase in temperature, which leads to a noticeable increase in the Full Width Half Maximum, *FWHM* and *d*-spacing (in Å). According to Bragg's law ($\lambda=2d\cdot\mathrm{Sin}\phi$), the *d*-spacing has an inverse relation with 2ϕ, where $\lambda$ is the wavelength and *d* is the lattice spacing. It should be noted that the shift in the peaks and the change in the *d*-spacing (refer Table 9) are indications of the structural transformation(s) in the soil due to its exposure to elevated temperatures [65]. Furthermore, from Fig. 8, it can be seen that the peak position 2ϕ is different for various types of soils. However, the soils with the same mineralogy (viz., Soils S2 and S3) exhibit similar peaks as well as a similar shift in peaks with respect to the temperature. It should also be noted that the intensities (peak areas) of the different peaks, for a mineral, commonly vary due to the specific structural and compositional effects of the unit cell on the diffracted beam of the X-ray. Hence, due to an increase in temperature there is an increase in the thermal vibration of the lattice, which can be attributed to a decrease in the intensity of the diffracted beam [66]. These changes in the crystallographic characteristics strongly influence the physical and chemical properties of the soil. Thus, the changes in *d*-spacing can be attributed to the expansion of the minerals due to the exposure of the soil to elevated temperatures.

## 7.9 LINEAR EXPANSION

It can be observed from the trends shown in Fig.1 that with an increase in temperature, θ, the *PLE* either decreases (a negative value corresponds to shrinkage) or increases (a positive value corresponds to expansion), depending upon the soil type. The Soils BT, S1, S2 and S3 exhibit shrinkage, which could be attributed to a reduction in the double layer, due to a loss of hygroscopic moisture, from the soils containing montmorillonite as active minerals. In contrast, the Soils S4 and WC, containing passive minerals (viz., quartz and kaolinite), exhibit expansion due to heating. It is worth mentioning here that the hygroscopic moisture, which is the water held tightly on the surface of soil particles (due to the presence of active minerals), does not evaporate at normal temperatures [67].

**Table 9**. The *d*-spacings of various samples at elevated temperatures.

| θ (°) | *d*-spacing (nm) | | | | | |
|---|---|---|---|---|---|---|
| | BT | WC | S1 | S2 | S3 | S4 |
| 30 | 0.197373 | 0.358977 | 0.335119 | 0.337032 | 0.339574 | 0.334133 |
| 50 | 0.197344 | 0.359352 | 0.335226 | 0.337191 | 0.339729 | 0.334166 |
| 100 | 0.197457 | 0.359623 | 0.33543 | 0.337381 | 0.339932 | 0.334382 |
| 150 | 0.197544 | 0.359958 | 0.335621 | 0.337523 | 0.340088 | 0.334499 |
| 200 | 0.197587 | 0.360226 | 0.335873 | 0.337826 | 0.340334 | 0.334717 |
| 250 | 0.197678 | 0.360693 | 0.336159 | 0.338061 | 0.340675 | 0.335048 |
| 300 | 0.197559 | 0.360843 | 0.336405 | 0.338402 | 0.340904 | 0.335307 |

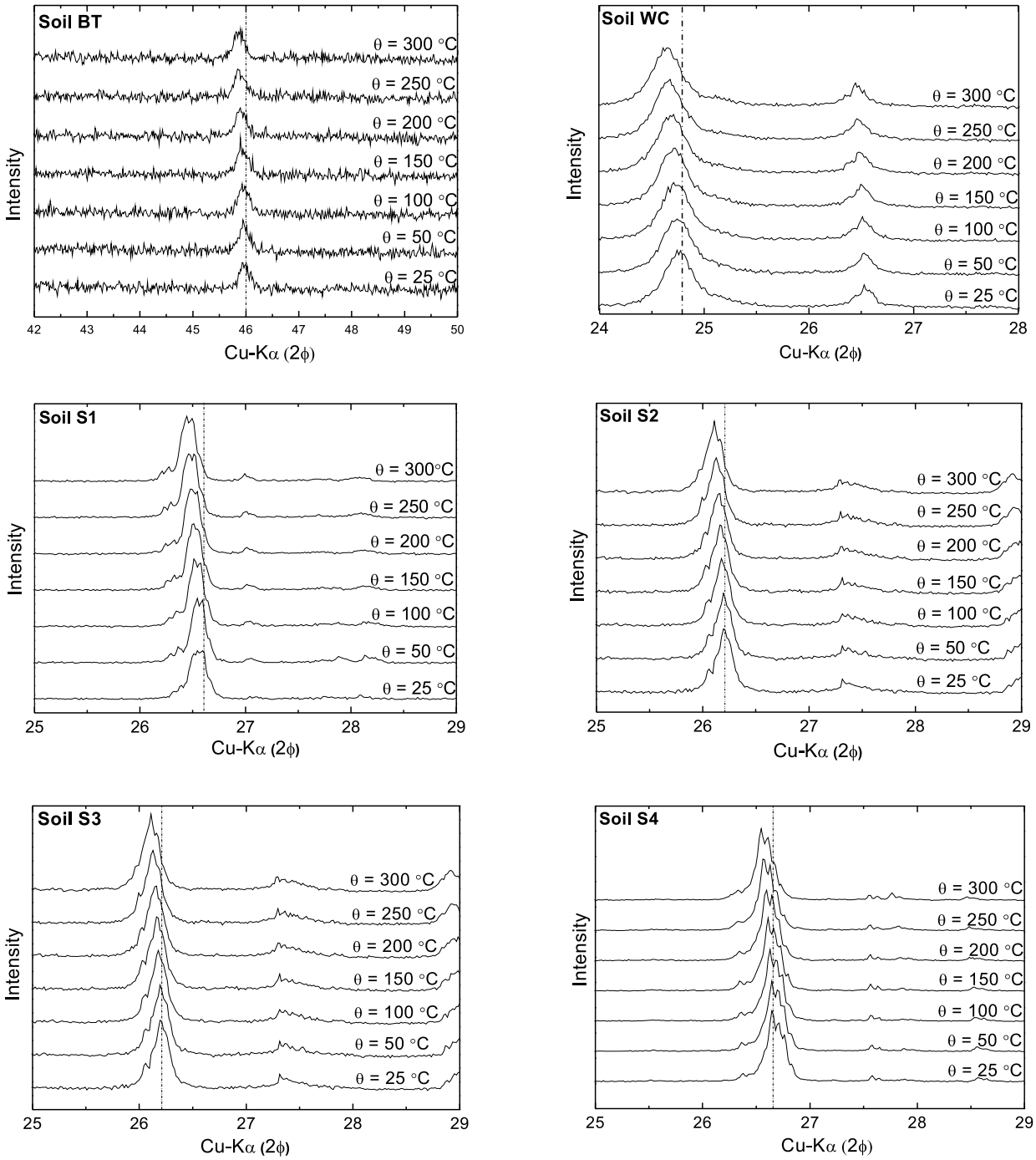


**Figure 8**. X-Ray Diffractograms of the investigated soils heated at different temperatures.

## 7.10 THERMO GRAVIMETRIC ANALYSIS (TGA)

The results of the TGA for different soil samples in an inert atmosphere (i.e., nitrogen gas, $N_2$) are depicted in Fig. 9. The samples were subjected to a thermal treatment only up to 300°C, in view of the fact that even in deep geological formations (repositories) the rise in temperature will not exceed 300°C. From the trends shown in Fig. 9, it is clear that at 50°C, as expected, no

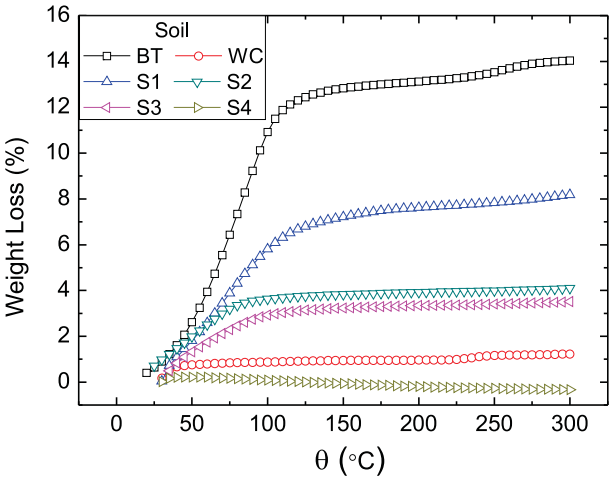


**Figure 9**. Variation of the weight loss of the investigated soils with temperature.

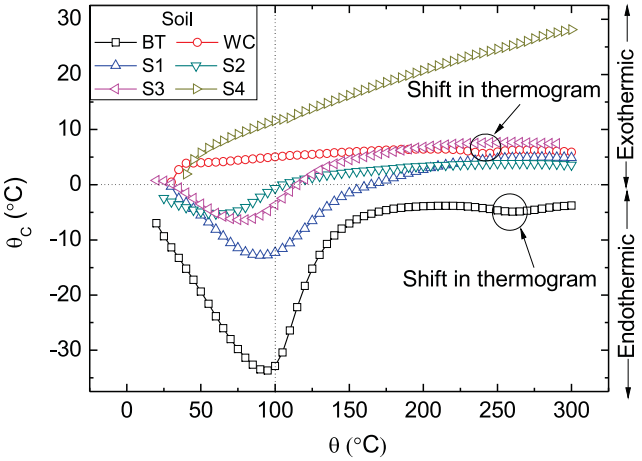


**Figure 10**. Variation of the temperature difference between the reference material and the soils at elevated temperatures.

appreciable change in the weight of the soil is observed except for the soil BT. This can be attributed to the fact that the thermal energy corresponding to this temperature is not sufficient to cause a significant weight loss of the soil sample. However, a very rapid weight loss in the soil sample was observed corresponding to 50–100°C, which can be attributed to the loss of weakly bonded hygroscopic moisture content, sorbed on the soil particles. While, between 100 to 300°C, a steady weight loss was observed, which might be attributed to the loss of the adsorbed water from the interlayer (containing cations) of the soil particles. Incidentally, it can also be observed from the figure that the weight loss for θ>150°C is almost constant, except for the Soil S4, due to its mineralogy and particle size.

In general, Fig. 9 substantiates the fact that the loss of weight is much more for the Soil BT than for its counterparts, which could be attributed to the presence of a higher clay fraction and active minerals (as listed in Tables 1 and 5) that would result in a larger hygroscopic moisture content [67]. Usually, a loss in weight of the soil sample can be attributed to the escape of volatiles and moisture, when $N_2$ (inert atmosphere) is used for combustion. Thus, the loss of weight of these soils can be attributed to a release of moisture and the oxidation of carbon compounds present in them. Incidentally, the Soil WC, though it contains a higher percentage of clay, exhibits a low percentage of weight loss due to the presence of the passive mineral (Kaolinite, refer Table 5). Furthermore, Soil S4 (i.e., the fine sand) exhibits a smaller percentage of the weight loss due to its passive nature as listed in Table 5 (viz., the presence of the passive mineral, quartz) and the negligible percentage of clay content.

## 7.11 DIFFERENTIAL THERMAL ANALYSIS (DTA)

The results obtained from the *DTA* for the soils in an inert atmosphere (with $N_2$) are plotted as a variation in temperature with respect to the reference material (i.e., Alumina), designated as $\theta_c$, versus the exposure temperature, θ, as shown in Fig. 10. It can be seen from this figure that the combustion of the soil may result in both exothermic as well as endothermic reactions, due to the physical and chemical changes occurring in it. In general, for soils, endothermic reactions occur due to dehydration, dehydroxylation, structural decomposition, sintering and melting, or evaporation and sublimation, whereas exothermic reactions may occur due to oxidation/burning of the organic matter, iron oxidation, or the crystallization of amorphous material [68]. In this context, it can be seen from Fig. 10 that the Soils BT, S1, S2 and S3 exhibit a more endothermic reaction as compared to their counterparts (viz., Soils WC and S4). This can be attributed to the lower heat-holding capacity of the Soils WC and S4, which exhibit a lower percentage weight loss as compared to their counterparts (see Fig. 9). Furthermore, Soils BT and S1 exhibit an endothermic reaction (i.e., heat absorption) up to 100°C due to the presence of hygroscopic moisture and thereafter a reduction in the endothermic reaction due to the loss of moisture. According to Barshad [69], the removal of the crystal lattice water (dehydroxylation) causes a complete destruction of the mineral structure and hence the dehydration reactions are endothermic. Furthermore, a slight shift from the regular trend has been observed in the thermogram of the Soils BT and WC, as shown in Fig. 10. This reveals the structural change undergone

by the crystal structure of these soils at θ≈250°C, which can be observed by a large shift in the peaks at 250°C, as shown in Fig. 8. The structural changes can also be attributed to the process of drying, which results in the shrinkage (refer Fig. 1) and formation of fissures that could introduce thermal resistance in the fine-grained soils. Furthermore, the fragmentation of these soils leads to the generation of air gaps, which is responsible for a decrease in the thermal conductivity.

## CONCLUSIONS

Based on a critical synthesis of the results and the discussion presented in the preceding sections, the following can be concluded.

1. The change in the color of the soil for θ≤250°C can be attributed to the depletion of the organic matter, while for θ>250°C the same can be attributed to increased oxidation and chemical changes, except for the soil WC.
2. An increase in the specific gravity and a decrease in the specific surface area of the soil, due to its exposure to elevated temperatures, was observed. This can be attributed to a depletion in the moisture and agglomeration of the fine organic matter present in the soil.
3. It has been observed that, except for the soils with passive minerals, the clay-sized fraction decreases, while the silt-sized fraction increases with an increase in temperature. This further substantiates the fact that the exposure of the soil to elevated temperatures results in an increase in its particle size.
4. The decrease in the specific surface area of the soil can be further substantiated by an increase in its particle size due to its exposure to elevated temperatures. This phenomenon was demonstrated by laser scanning diffraction analyses.
5. A reduction in exchangeable cations and a loss of organic matter results in a decrease in the cation--exchange capacity of the soils when they are exposed to higher temperatures.
6. A reduction in the zeta-potential of the soil has been noted due to its exposure to elevated temperatures.
7. The study demonstrates that with an increase in exposure temperature, there is a change in the lattice spacing, which indicates structural transformation. These changes in the crystallographic characteristics strongly influence the physical and chemical properties of the soil.
8. It has been observed that with an increase in temperature, the soils containing passive minerals (viz., quartz and kaolinite), exhibit an expansion. In contrast, soils containing active minerals (viz., montmorillonite) shrink, due to the loss of hygroscopic moisture.

In the authors' opinion, these changes to the soil properties, due to the exposure to elevated temperatures, would be quite important and crucial for designing various structures (viz., liners of waste landfills and cores of the dams, which are primarily constructed from fine-grained soils, treatment and the stabilization of highly contaminated soils and dredged sediments, the stabilization of weak foundation soils, the construction of roads and airfields, based on thermal stabilization).

## REFERENCES

[1] Li, Y., Wang, L. and Liu, L. (2011). Study on constructional reinforcement for the foundation of blast furnace due to temperature effect. *International Conference on Civil Engineering and Transportation*, ICCET, Vol. 94-96, pp. 1545-1548.

[2] Gangadhara Rao, M.V.B.B. and Singh, D.N. (1999). A generalized Relationship to Estimate Thermal Resistivity of Soils. *Canadian Geotechnical Journal*, Vol. 36, No. 4, pp. 767-773.

[3] Varlakov, A., Sobolev, I., Barinov, A., Dmitriev, S., Karlin, S. and Flit, V. (1997). Method of treatment of radioactive silts and soils. Proceedings of the MRS Fall Meeting, Moscow, Russia, *Materials Research Society*, Pittsburgh, PA, pp. 591-594.

[4] Farag, I. (1993). Simulating hazardous waste incineration. *Chemical Engineer*, Issue-538, pp. 11-16.

[5] Ma, C. and Hueckel, T. (1992). Stress and pore pressure in saturated clay subjected to heat from radioactive waste: a numerical simulation. *Canadian Geotechnical Journal*, Vol. 29, pp. 1087-1094.

[6] Alcocer, C. and Chowdhury, H. (1993). Experimental study of an environmental remediation of Gulf Coast crude-oil contaminated soil using low temperature thermal treatment. *Proceedings of the Western Regional Meeting, Louisiana, Society of Petroleum Engineers,* Richardson, pp. 723-724.

[7] Akinmusuru, J. (1994). Thermal conductivity of earth blocks. *Journal of Materials in Civil Engineering*, Vol. 6, No. 3, pp. 341-351.

[8] Joshi, R., Achari, G.C., Horsfield, D. and Nagaraj, T. (1994). Effect of heat treatment on strength of clays. *Journal of Geotechnical Engineering*, Vol. 120, No. 6, pp. 1080-1088.

[9] Yang, L. and Farouk, B. (1995). Modelling of solid particles flow and heat transfer in rotary kiln calciners. *Proceedings of the 30th National Heat*

*Transfer Conference*, Portland, Oregon, American Society of Mechanical Engineers, New York, NY, pp. 11-19.

[10] Krishnaiah, S. and Singh, D.N. (2006). Determination of Thermal Properties of Soils in a Geotechnical Centrifuge. *Journal of Testing and Evaluation*, ASTM, Vol. 34, No. 4, pp. 1-8.

[11] Litvinov, I.M. (1906). Stabilization of settling and weak clayey soils by thermal treatment. *Highway research board special report 60*, National Research Council, Washington, DC, pp. 94-112.

[12] Mitchell, J.K. (1969). Temperature effects on the engineering properties and behavior of soils. *Highway Research Board Special Report* 103, Washington, DC, pp. 9-28.

[13] Ketterings, Q.M., Bigham, J.M. and Laperrche, V. (2000). Changes in soil mineralogy and texture caused by slash and burn fires in Sumatra, Indonesia. *Soil Science Society of American Journal*, Vol. 64, pp. 1108-1117.

[14] Ulery, A.L. and Graham, R.C. (1993). Forest fire effects on soil color and texture. *Soil Science Society of American Journal*, Vol. 57, pp. 135-140.

[15] Sertsu, S.M. and Sanchez, P.A. (1978). Effects of heating on some changes in soil properties in relation to an Ethiopian land management practice. *Soil Science Society of American Journal*, Vol. 42, pp. 940-944.

[16] Fernandez, I., Cabaneiro, A. and Carballas, T. (1997). Organic matter changes immediately after a wildfire in an Atlantic forest soil comparison with laboratory soil heating. *Soil Biology Biochemistry*, Vol. 29, pp. 1-11.

[17] Yilmaz, G. (2011). The effects of temperature on the characteristics of Kaolinite and Bentonite. *Academic Journals, Scientific Research and Essays*, Vol. 6, No. 9, pp. 1928-1939.

[18] Utkaeva, V. F. (2007). Specific surface area and wetting heat of different soil types in European Russia. ISSN 1064-2293, *Eurasian Soil Science*, Pleiades Publishing, Ltd., Vol. 40, No. 11, pp. 1193-1202.

[19] Abu-Zreig, M.M., Al-Akhras, N.M. and Attom, M.F. (2001). Influence of heat treatment on the behavior of clayey soils. *Applied Clay Science*, Vol. 20, pp. 129-135.

[20] Tan, O., Yilmaz, L. and Zaimoglu, A.S. (2004). Variation of some engineering properties of clays with heat treatment. *Materials Letters*, Vol. 58, No. 7-8, pp. 1176-1179.

[21] Sultan, N., Delage, P. and Cui, Y.J. (2002). Temperature effects on the volume change behavior of Boom clay. *Engineering Geology*, Vol. 64, pp. 135-145.

[22] Parlak, M. (2011). Effect of heating on some physical, chemical and mineralogical aspects of forest soil. Bartin Orman Fakultesi Dergisi, Cilt: 13, Sayi, 19, pp. 143-152.

[23] Ghuman, B.S. and Lal, R. (1989). Soil temperature effects of biomass burning in windrows after clearing a tropical rainforest. *Field Crops Research*, Vol. 22, pp. 1-10.

[24] Certini, G. (2005). Effects of fire on properties of forest soils. *A review of Oecologia*, Vol. 143, pp. 1-10.

[25] Hatten, J., Zabowski, D., Scherer, G. and Dolan, E.A. (2005). Comparison of soil properties after contemporary wildfire and fire suppression. *Forest Ecology and Management*, Vol. 220, No. 1-3, pp. 227-241.

[26] Moritz, L. and Gabrielsson, A. (2000). Temperature effect on the properties of clay. *Soft ground Technology conference,* ASCE, pp. 304-314.

[27] Tanaka, N., Graham, J. and Crilly, T. (1997). Stress-strain behaviour of reconstituted illitic clay at different temperatures. *Engineering Geology*, Vol. 47, pp. 339-350.

[28] Zhang, Y., Miao, L., and Wang, F. (2011). Study on the engineering properties of the stabilized mucky clay as backfill material in highway embankment projects. *Geo-Frontiers 2011: Advances in Geotechnical Engineering*, ASCE, pp. 1365-1371.

[29] Booker, J.R., and Savvidou, C., (1985). Consolidation Around a point heat source. *International Journal of Numerical and Analytical Methods in Geomechanics*, Vol. 9, pp. 173-184.

[30] Varlakov, A., Sobolev, I., Barinov A., Dmitriev S., Karlin S., Flit V. (1997). Method of Treatment of Radioactive Silts and Soils. *Proceedings of the MRS Fall Meeting*, Moscow, Russia, Materials Research Society, Pittsburgh, PA, 591-594.

[31] ASTM D 5550-06, Standard test method for specific gravity of soil solids by gas pycnometer. *Annual Book of ASTM Standard*, 04.08, ASTM, Philadelphia, USA.

[32] ASTM D 422-63, Standard test method for particle size analysis of soils. *Annual Book of ASTM Standards*, 04.08, ASTM, Philadelphia, USA, 1994.

[33] Eshel, G., Levy, G.J, Mingelgrin, U. and Singer M.J. (2004). Critical evaluation of the use of laser diffraction for particle-size distribution analysis. *Soil Science Society American Journal,* Vol. 68, pp. 736-743.

[34] Stanley, J.V. and Leon Y.S. (1997). Particle-size analysis of soils using laser light scattering and X-Ray absorption technology. *Geotechnical Testing Journal*, Vol. 20, No. 1, pp. 63-73.

[35] Beverwijk, A. (1967). Particle size analysis of soils

by means of the hydrometer method. *Sediment. Geol.*, Vol. 1, pp. 403-406.

[36] Konert, M., and Vandenberghe, J. (1997). Comparison of laser grain size analysis with pipette and sieve analysis: a solution for the underestimation of the clay fraction. Sedimentology, Vol. 44, pp. 523-535.

[37] Bah, A.R., Kravchuk, O., and Kirchhof, G. (2009). Fitting performance of particle-size distribution models on data derived by conventional and laser diffraction techniques. *Soil Science Society America Journal*, Vol. 73, pp. 1101-1107.

[38] Shanthakumar, S., Singh, D.N. and Phadke, R.C. (2010). Methodology for Determining Particle-Size Distribution Characteristics of Fly Ashes. *Journal of Materials in Civil Engineering*, ASCE, VOl. 22(5), pp. 435-442.

[39] ASTM D 4318-93, Standard test method liquid limit, plastic limit and plasticity index of soils. *Annual Book of ASTM Standards*, 04.08, ASTM, Philadelphia, USA, 1994.

[40] ASTM D 427, Test Method for shrinkage factors of soils by the mercury method. *Annual Book of ASTM Standards*, 04.08, ASTM, Philadelphia, USA.

[41] ASTM D 2487-10, Standard practice for classification of soils for engineering purposes (Unified Soil Classification System). *Annual Book of ASTM Standards*, 04.08, ASTM, Philadelphia, USA.

[42] Carter, D.L., Mortland, M.M. and Kemper, W.D. (1986). Specific Surface-Methods of Soil Analysis, *American Society of Agronomy*, USA, pp. 412-423.

[43] Cerato, A.B. and Lutenegger, A.J. (2002). Determination of surface area of fine grained soils by the ethylene glycol mono-ethyl ether (EGME) method. *Geotechnical Testing Journal*, ASTM, Vol. 25, No. 3, pp. 1-7.

[44] Arnepalli, D.N., Shanthakumar, S., Hanumantha, Rao, B. and Singh, D.N. (2008). Comparison of methods for determining specific-surface area of fine-grained soils. *Geotech Geol Eng*, Vol. 26, pp. 121-132.

[45] Kyziol, J., (2002). Effect of physical properties and cation exchange capacity on sorption of heavy metals onto peats. *Journal of Environmental Studies*, Vol. 11(6), pp. 713-718.

[46] Liu, X. and Lu, X. (2011). Correlation between Bentonite's Cation Exchange Capacity (CEC) activated clay quality indexes and activation strength. *Applied Mechanics and Materials*, Vol. 99-100, pp. 1031-1034.

[47] IS 2720 Part XXIV (1976). Methods of test for soils determination of cation exchange capacity. *Indian Standards Institute*, New Delhi, India.

[48] Sparks, D.L. (1986). Soil Physical Chemistry, CRC Press, Boca Raton

[49] West, L.J. and Stewart, D.L. (1995). Effect of zeta potential on soil electrokinesis. *Proceedings of Geoenvironment*, ASCE Special Publication, pp. 1535-1549.

[50] Vane, L.M. and Zhang, G.M. (1997). Effects of aqueous phase properties on clay particle zeta potential and electro-osmotic permeability: Implications for electro kinetic soil remediation processes. *Journal of Hazardous Materials*, Vol. 55, No. 1-3, pp. 1-22.

[51] Yukselen, Y. and Kaya, A. (2003). Zeta potential of Kaolinite in the presence of alkali, alkaline earth and hydrolyzable metal ions. *Journal of Water, Air and Soil Pollution*, Vol. 145, No. 1-4, pp. 155-168.

[52] Kaya, A., Oren, A.H. and Yukselen, Y. (2003). Settling behaviour and zeta potential of Kaolinite in aqueous media. *Proceedings of the Thirteenth International Offshore and Polar Engineering Conference Honolulu*, Hawaii, USA, pp. 407- 412.

[53] Kaya, A. and Yukselen, Y. (2005). Zeta potential of clay minerals and quartz contaminated by heavy metals. *Canadian Geotechnical Journal*. Vol. 42, No. 5, pp. 1280-1289.

[54] Cox, R.J., Peterson, H.L., Young, J., Cusik, C. and Espinoza, E.O. (2000). The forensic analysis of soil organic by FTIR. *Forensic science International*, Vol. 108, pp. 107-116.

[55] Ivan, S., Pavel, D., Stefan, D.H., Mataix-Solera, J. and Vlasta, S. (2008). Thermal destruction of soil water repellency and associated changes to soil organic matter as observed by FTIR spectroscopy. *Catena*, Vol. 74, pp. 205-211.

[56] JCPDS (1994). Power diffraction file, 44, 7354-CD ROM (PDF 1-44), International Centre for Diffraction Data, Pennsylvania

[57] Young, R.A. (2002). The Rietveld Method. International Union of Crystallography, *Oxford University Press*, New York, NY.USA.

[58] Young, R.A., Larson, A.C., and Paiva-Santos, C.O. (2000). User's guide to program DBWS-9807a for Rietveld analysis of X-ray and neutron powder diffraction patterns. *Georgia Institute of Technology*, Atlanta, GA, USA.

[59] Grim, R. E., and Rowland, R. A. (1944). Differential thermal analysis of clays and shales, control and prospecting method. *American Ceramic Society Journal*, Vol. 27, pp. 65-76.

[60] Allaway, W. H. (1948). Differential thermal analyses of clays treated with organic cations as an aid in the study of soil colloids. *Soil Science Society of America Proc*, Vol. 13, pp. 183-188.

[61] Kampf, N., Scheinost, A.C. and Schulze, D.G. (2000). Oxide minerals. In: M.E. Sumner (Ed.), Handbook of Soil Science, CRC Press: Boca Raton, Fl., pp. 125-165.
[62] Schwertmann, U. (1984). The double dehydroxylation peak of goethite, *Thermochimica Acta*, Vol. 78, No. 1-3, pp. 39-46.
[63] Altinbaş, U. (1982). A study of the some properties of the raw material used in the ceramic industry at different temperatures. *Review of the Faculty of Agriculture*, University of Ege, Vol. 460, pp. 1-40.
[64] Chorom, M. and Rengasamy, P. (1996). Effect of heating on swelling and dispersion of different cationic forms of a smectite. *Clay and Clay Minerals*, Vol. 44, No. 6, pp. 783-790.
[65] Khameneh, A.S., Heydarzadeh, S.M. and Hadavi, S.M.M. (2004). The Effect of the Heat Treatment on Residual Stresses in HVOF Sprayed WC-Co Coating. *Materials Science Forum*, Vol. 465, No. 466, pp. 427-432.
[66] Cullity, B.D. and Stock, S.R. (2001). Elements of X-Ray Diffraction. 3rd Ed., Prentice-Hall Inc., ISBN 0-201-61091-4, pp. 167-171.
[67] Shah, P.H. and Singh, D.N. (2006). Methodology for Determination of Hygroscopic Moisture Content of Soils. *Journal of ASTM International*, Vol. 3, No. 2, pp. 1-14.
[68] Smykatz-Kloss, W., (1982). Application of differential thermal analysis in mineralogy. *Journal of Thermal Analysis*, Vol. 23, No. 1-2, pp. 15-44.
[69] Barshad, I. (1995). Thermal analysis techniques for mineral identification and mineralogical composition. *Methods of soil analysis, Agronomy*, American Society of Agronomy, Madison, Wisc. No. 9, Chapter 50.